

Dynamic performance analysis of lasing mode optical integrated device

Sh. M. Eladl, K. A. Sharshar, M. H. Saad

Radiation Engineering Dept. National Center for Radiation Research and Technology (NCRRT),
Egyptian Atomic Energy Authority (EAEA), Nasr City, Cairo, Egypt
E-mail: shaban_45@yahoo.com; ksharshar@yahoo.com

Abstract. In this paper, the dynamic response of the optical gain of optical integrated device composed of a heterojunction bipolar transistor (HBT) and a laser diode (LD) has been numerically analyzed. This type of optical integrated device is called transistor laser (TL). First, the rate equation of LD has been solved to obtain its transfer function. Second, the overall transfer function of the whole structure has been analyzed numerically. The effect of HBT cutoff frequency on the amplitude and phase frequency response has been studied. The obtained results show that HBT has a strong influence on the device performance. In particular, higher values of HBT cutoff frequency result in lower amplitudes and higher phase values in the low-frequency range. The device is stable and has a fast response and high optical gain at higher frequencies. Therefore, it can be used as an optical amplifier or optical switch in high-speed optical systems.

Keywords: optical integrated device, laser diode, heterojunction bipolar transistor, transistor laser, heterojunction bipolar transistor laser, heterojunction bipolar light emitting transistor.

<https://doi.org/10.15407/spqeo25.02.196>
PACS 07.57.Kp, 85.35.Be, 85.60.Dw, 85.60.Jb

Manuscript received 18.09.21; revised version received 03.06.22; accepted for publication 22.06.22; published online 30.06.22.

1. Introduction

First inventions of TLs were proposed in [1, 2]. A great interest of both experimental and theoretical researchers is attracted to the study of heterojunction bipolar transistor lasers (HBTLs), also known as transistor lasers (TL) [3–6]. Integration of lasers and transistors is an effective method to obtain multifunctionality of optical signal processing. TLs are the key elements for optical signal processing applications to achieve large bandwidths, frequency multiplication, nonlinear signal mixing, and negative resistance. They are widely used in opto-electronic logic gates [7].

TL operation can be explained as follows. Input electrical signal to be amplified by the transistor comes from the emitter layer through a thin base to the collector layer. The transistor switches laser diode (LD) to on state with intense light power. Sometimes, such optical integrated device contains a quantum well (QW) incorporated in the base of heterojunction bipolar transistor (HBT). The concentration of injected carriers is sufficient to create population inversion between the conduction and the valence subbands of QW and to make the optical gain overcoming the material and mirror losses [8, 9]. TL operates as a typical transistor but emits

optical signals through one of its output windows rather than provides electrical output. A cavity within the device focuses generated light into a laser beam. The hetero-junction bipolar transistor with a quantum well may be considered to increase the intensity of output light in its base region.

The characteristics of heterojunction bipolar transistor lasers such as optical frequency response and current gain (β) can be enhanced by optimizing their parameters [10]. In this paper, the frequency response of an optical integrated device composed of HBT and LD is analyzed theoretically. The motivation behind this work is the need to examine the usability of HBTLs as optical functional devices for optical communication systems.

A transistor laser was composed of indium gallium phosphide (InGaP), gallium arsenide (GaAs) and indium gallium arsenide (InGaAs) layers, which enabled it to operate without cooling. A number of interesting features were demonstrated for such TL, including resonance-free frequency response, large direct modulation bandwidth [11], voltage-controlled mode of operation, and low relative intensity noise (RIN) [12]. The transistor laser offers some advantages, namely: better modulation bandwidth, reduced chirp, and minimum relative intensity noise.

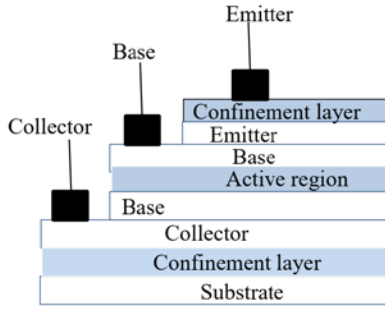


Fig. 1. Schematic structure of transistor laser.

This paper is organized as follows. The device structure and theoretical modeling including solution of laser diode rate equation and analysis of the overall transfer function are presented in Section 2. Obtained results and curves of amplitude and phase response at different values of HBT cutoff frequency are presented in Section 3. Conclusion and future work plans are outlined in Section 4.

2. Theoretical analysis

2.1. Structure and operation of the device

The schematic view of TL structure composed of HBT and LD is shown in Fig. 1. HBT contains n -InGaP and p -GaAs base layers as well as an n -type heavy doped collector layer. The active layer of LD is single QW of i -InGaAs. The carriers injected in QW are captured very fast causing activation of TL [10].

2.2. Dynamic behaviour

To understand the response of the device to a small signal with a frequency ω , we write the photon and carrier density rate equations as follows [13, 14]:

$$\frac{dP}{dt} = GP + R_{sp} - \frac{P}{\tau_c}, \quad (1)$$

$$\frac{dN}{dt} = GP + \frac{I}{q} - \frac{N}{\tau_c}, \quad (2)$$

where R_{sp} – rate of spontaneous emission in lasing mode, τ_p – photon lifetime, τ_c – carrier lifetime, G – net rate of stimulated emission, I – intensity of the current applied to the laser diode, and q is the elementary charge, p is optical power and N is the carrier density.

In the small-signal limit, the current signal is assumed to be as follows:

$$I = I_0 + \delta I e^{j\omega t}, \quad (3)$$

which causes the following variations in the carrier and the photon densities:

$$N = N + \delta N e^{j\omega t}, \quad (4)$$

$$P = P + \delta P e^{j\omega t}. \quad (5)$$

The gain and spontaneous rate can be linearized as follows:

$$G = G_b + \frac{dg}{dN} \delta N - \frac{N}{\tau_c}, \quad (6)$$

$$R_{sp} = R_{sp}(N) + \frac{R_{sp}}{dN} \delta N. \quad (7)$$

After substituting the small signal variations into the rate equations, retaining only the first-order small signal terms and eliminating δN , the relation between the photon signal δP and the current signal δI becomes

$$\frac{\delta P}{\delta I} = R_{LD}(\omega) = \frac{(2\pi f_r)^2}{((2\pi f_r)^2 - \omega^2 + J\omega\gamma)}. \quad (8)$$

Here,

$$(f_r)^2 = \frac{1}{4\pi^2} \left[\frac{1}{\tau_p} \frac{dR_{sp}}{dN} + \frac{P_0}{\tau_p} \frac{dg}{dN} \right] \quad (9)$$

and

$$\gamma = 4\pi^2 (f_r)^2 \tau_p. \quad (10)$$

The transfer function of HBT can be obtained from [9] in the following form:

$$R_{HBT}(\omega) = \frac{\beta_0}{J2\pi f + 2\pi f_b}, \quad (11)$$

where β_0 is the common emitter current gain and f_b is the HBT cutoff frequency, respectively.

The overall transfer function of HBT/LD can be obtained from Eqs. (8) and (11) as follows:

$$G(\omega) = R_{LD}(\omega) \times R_{HBT}(\omega) = \frac{\beta_0}{J2\pi f + 2\pi f_b} \cdot \frac{(2\pi f_r)^2}{((2\pi f_r)^2 - (2\pi f)^2 + J(2\pi f)\gamma)}. \quad (12)$$

The amplitude of the expression (12) is

$$|G(\omega)| = |R_{LD}(\omega) \times R_{HBT}(\omega)| = \frac{\beta_0}{\sqrt{(2\pi f)^2 + (2\pi f_b)^2}} \cdot \frac{(2\pi f_r)^2}{\sqrt{((2\pi f_r)^2 - (2\pi f)^2)^2 + (2\pi f\gamma)^2}}. \quad (13)$$

Its magnitude is given by

$$|G(\omega)|_{dB} = 20 \log_{10} \frac{\beta_0}{\sqrt{(2\pi f)^2 + (2\pi f_b)^2}} \times \frac{(2\pi f_r)^2}{\sqrt{((2\pi f_r)^2 - (2\pi f)^2)^2 + (2\pi f\gamma)^2}}. \quad (14)$$

The phase is calculated as follows:

$$\phi = \angle G(\omega) = \tan^{-1}(R_{LD}(\omega)) + \tan^{-1}(R_{HBT}(\omega)). \quad (15)$$

Therefore,

$$\varphi = \tan^{-1}\left(\frac{f_b}{f}\right) + \tan^{-1}\left(\frac{(2\pi f_r)^2}{((2\pi f_r)^2 - (2\pi f)^2)}\right). \quad (16)$$

To obtain the transient response of the optical gain of TL device, Eq. (12) must be transformed into the time-domain one using Fourier or Laplace Transform after setting $s = J2\pi f$:

$$G(t) = \mathcal{L}^{-1}G(s) = \mathcal{L}^{-1}\left[\frac{\beta_0}{s + 2\pi f_b} \cdot \frac{(2\pi f_r)^2}{((2\pi f_r)^2 - (s)^2 + J(s)\gamma)}\right], \quad (17)$$

where $G(s)$ is the Laplace Transform of $G(t)$.

The following expression is obtained after all transformations:

$$G(t) = \beta_0 \left\{ 1 + \frac{(f_r)^2 e^{-f_b t} \cosh\left(\frac{t\sqrt{\gamma^2 - 4(f_r)^2}}{2}\right) e^{-\frac{\gamma t}{2}(f_b - \gamma)f_b}}{f_b \gamma - (f_r)^2 - (f_b)^2} \right\} + \beta_0 \left\{ \frac{(f_r)^2 e^{-f_b t} \sinh\left(\frac{t\sqrt{\gamma^2 - 4(f_r)^2}}{2}\right) e^{-\frac{\gamma t}{2}(-f_b \gamma - 2(f_r)^2 + \gamma^2)f_b}}{(-f_b \gamma + (f_r)^2 + (f_b)^2)\left(\sqrt{\gamma^2 - 4(f_r)^2}\right)} \right\}. \quad (18)$$

3. Results and discussions

The values of device parameters used in the calculations are as follows: $f_b = 0.1$ GHz, $\gamma = 0.01$ GHz, $\beta = 100$, and $f_r = 3$ GHz. The amplitude response of the optical gain of HPT/LD at different values of HBT cutoff frequency is shown in Fig. 2. It can be seen from this figure that the amplitude of HPT/LD has a constant value in the low-frequency range. It should be noticed as well that the data presented by the plot in Fig. 2 are calculated for the first-order low-pass filter mode of LED operation. In this mode, the overall transfer function consists of two terms, each term being a first-order low-pass filter. The amplitude of one term depends on the HBT cutoff frequency, while the amplitude of the other one depends on the damping frequency. It can be also seen from Fig. 2 that the amplitude linearly decreases with the increase of frequency in the higher-frequency range. At this, the amplitude is lower and the bandwidth is larger at higher cutoff frequencies.

The phase response of the developed optical device is obtained by measuring the relationship between the phases of input and generated output signal. The phase response of the optical gain of HPT/LD at different values of HBT cutoff frequency for the LED

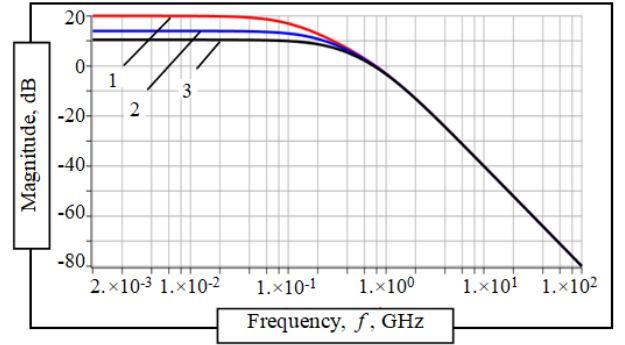


Fig. 2. LED mode magnitude response of HPT/LD at different values of HBT cutoff frequency. 1(red) – $f_b = 0.1$ GHz, 2(blue) – 0.2 GHz, 3(black) – 0.3 GHz. (Color online)

mode operation of laser diode is shown in Fig. 3. It can be seen from this figure that the phase of the device gradually decreases from zero value at the frequencies close to the HBT cutoff one and reaches -180° at higher frequencies. The phase response increases with the increase of HBT cutoff frequency at frequencies close to it. Obtained results have a good agreement with the results of the measurements of the frequency response of TL operating in LED and lasing mode presented in [7, 15]. Operation of heterojunction bipolar light emitting transistor (HBLED) in LED mode was analyzed and the lasing mode was developed for a heterojunction bipolar laser transistor (HBLT) model.

The device operates in lasing mode when the resonance frequency is greater than the damping one. The amplitude response of the device operating in lasing mode versus frequency at different values of HBT cutoff frequency is shown in Fig. 4. It can be seen from this figure that at lower values of HBT cutoff frequency the amplitude is higher in the low-frequency range. The amplitude suddenly jumps to a peak value when the frequency is close to the resonant one. This peak directly depends on f_r , while the HBT cutoff frequency has

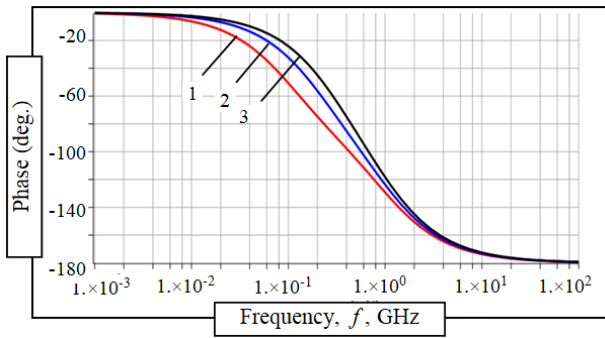


Fig. 3. LED mode phase response of HPT/LD at different values of HBT cutoff frequency. 1(red) – $f_b = 0.1$ GHz, 2(blue) – 0.2 GHz, 3(black) – 0.3 GHz. (Color online)

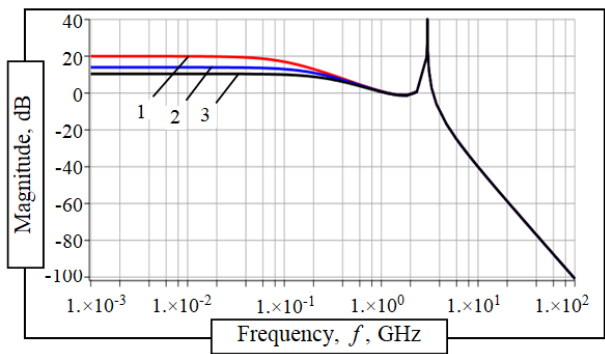


Fig. 4. Laser mode magnitude response of HPT/LD at different values of HBT cutoff frequency. 1(red) – $f_b = 0.1$ GHz, 2(blue) – 0.2 GHz, 3(black) – 0.3 GHz. (Color online)

no effect on it. At high frequencies, far away from the resonant one, the amplitude quickly decreases to the lowest value. These results have a good agreement with the results of the measurements of the frequency response of TL obtained in [16]. Improvement of amplitude response requires the increase of bias current. However, the resonance frequency and damping rate become eventually large, which limits the enhancement of device performance. Therefore, to achieve larger values of response at low bias currents, the differential gain should be high to reduce the damping effect and increase the resonant frequency at the same time.

Figure 5 shows the frequency dependence of the phase response of the device operating in lasing mode at different values of HBT cutoff frequency. It can be seen from this figure that the phase has a constant value up to the frequencies close to the HBT cutoff one and gradually decreases thereafter. The phase jumps down to the lowest value at the frequencies far away from the HBT cutoff one. The generated optical signal makes multiple round trips within the optical cavity before emerging. Each round trip causes loss of intensity and phase delay. The optical loss depends on the cavity length and its absorption properties. The phase delay is determined by the refractive index of the cavity region, operating wavelength and cavity length. Obtained results

concerning the phase variation with frequency in the LED and lasing mode show a good agreement with the measurement results presented in [17].

In the time domain, the transfer function (12) should be used to evaluate the transient response of TL devices. It should be transformed to the time domain by using any method like Fourier or Laplace Transform after setting $s = j2\pi f$. Transient behavior of optical output gain at different values of damping rate and lower values of HBT cutoff frequency is shown in Fig. 6. It can be seen from this figure that increase of damping frequency plays a major role in reducing the oscillatory peaks, while the lasing peaks of optical gain still have lower values as long as the HBT cutoff frequency is low. The transfer function for the device under study is considered as a third-order one with a single real and two complex conjugate roots. The dominant pole approximation scheme can be applied to this function. The device transfer function consists of three poles. The dominant pole is evaluated by comparing the value of the real root of HBT cutoff frequency f_b with the real part of the conjugate root of damping rate $\gamma/2$. Since $f_b = 0.5$ GHz and $\gamma/2$ ranges from 0.05 to 0.45 GHz, f_b is slightly greater than $\gamma/2$. This means that the complex conjugate root dominates and the time response starts to move toward the second order low pass filter scheme.

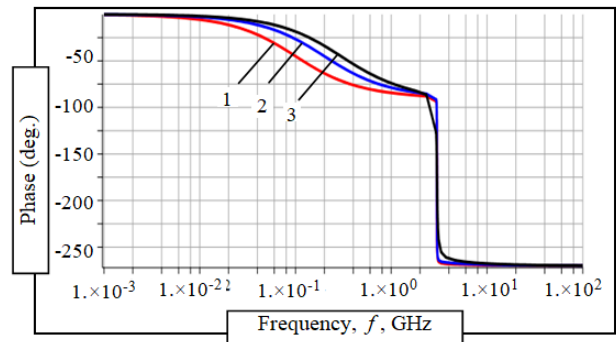


Fig. 5. Laser mode phase response of HPT/LD at different values of HBT cutoff frequency. 1(red) – $f_b = 0.1$ GHz, 2(blue) – 0.2 GHz, 3(black) – 0.3 GHz. (Color online)

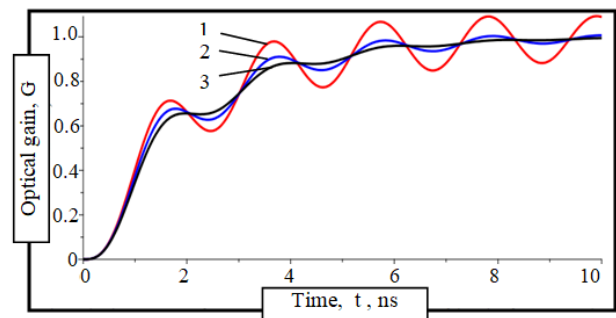


Fig. 6. Time response of optical output gain at different values of damping frequency and $f_b = 0.5$ GHz. 1(red) – $\gamma = 0.1$ GHz, 2(blue) – 0.5 GHz, 3(black) – 0.9 GHz. (Color online)

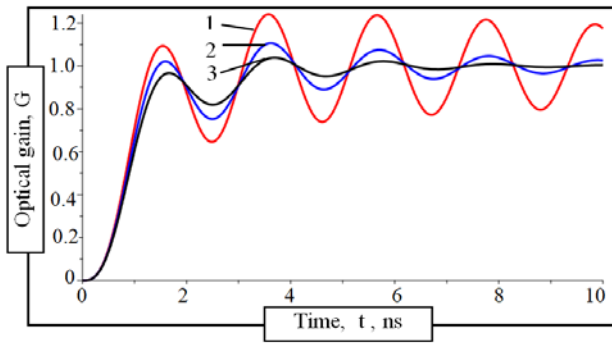


Fig. 7. Time response of optical output gain at different values of damping frequency and $f_b = 1$ GHz. 1 (red) – $\gamma = 0.1$ GHz, 2 (blue) – 0.5 GHz, 3 (black) – 0.9 GHz. (Color online)

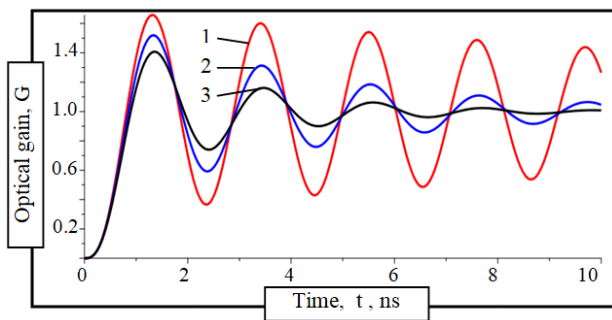


Fig. 8. Time response of optical output gain at different values of damping frequency and $f_b = 2$ GHz. 1 (red) – $\gamma = 0.1$ GHz, 2 (blue) – 0.5 GHz, 3 (black) – 0.9 GHz. (Color online)

As shown in Fig. 7, the oscillatory lasing peaks increase with the increase of HBT cutoff frequency and reach higher values without saturation. The TL device tends to reach the stable mode at higher values of damping frequency corresponding to the maximum peaks of the optical gain of 1.2. With the increase of HBT cutoff frequency from 0.5 to 1 GHz to notice the approximate response of the device, the value of HBT cutoff frequency is greater than the real value of the conjugate root, so the second order roots strongly dominates and the time response behaves like second order characteristic function with higher peaks and tend to produce the steady state stability.

Figure 8 shows transient behavior of optical gain at different values of damping rate and increased HBT cutoff frequency, $f_b = 2$ GHz. The device has higher value of gain up to 1.6 and improves short-time stability, which is beneficial for application of such devices in high-speed optical communication systems. The value of HBT cutoff frequency is larger than $\gamma/2$. Therefore, the complex conjugate root is dominating. The device operates in lasing mode and behaves like a second-order low-pass filter with better steady-state stability as compared to the cases considered above. Oscillations in time appear due to photons and carrier exchange in the active region of HBTTL caused by radiative recombination of electrons. At large resonance frequencies,

population inversion is created in the active region due to injection of the high concentrations of carriers. In the lasing mode, a significant amount of injected carriers is lost in the active region causing photon damping during subsequent photon emission.

4. Conclusion and future work

This paper is devoted to theoretical evaluation of the frequency response of the amplitude and phase of an optical integrated device. This device is composed of a heterojunction bipolar transistor and a laser diode and is called a transistor laser. The frequency dependences of amplitude and phase at different values of HBT cutoff frequency are analyzed. The frequency response strongly depends on the cutoff frequency and can be enhanced by its increase, which, however, leads to amplitude reduction. The transient response of this device at the HBT cutoff frequencies larger than the half of the damping rate corresponds to the lasing mode of device operation with second-order low-pass filter behavior. The opposite behavior is observed when the HBT cutoff frequency is lower than the half of the damping rate. Our study will be extended by analytical modeling of the temporal response of the device structure considered in this paper using its equivalent circuit. Since the developed transistor laser device reaches a steady-state high gain in a very short time, it is a good candidate for applications in fast and high-gain optical interconnection systems.

References

1. Feng M., Holonyak N., Jr., and Hafez W. Light-emitting transistor: Light emission from InGaP/GaAs heterojunction bipolar transistors. *Appl. Phys. Lett.* 2004. **84**, No 1. P. 151–153. <https://doi.org/10.1063/1.1637950>.
2. Feng M. Holonyak, N., Jr. The transistor laser. *IEEE Spectrum.* 2006. **43**, No 2. P. 50–55. <http://doi.org/10.1109/MSPEC.2006.1584362>.
3. Feng M., Qiu J., Wang C.Y., and Holonyak N., Jr. Tunneling modulation of a quantum-well transistor laser. *J. Appl. Phys.* 2016. **120**. P. 204501. <https://doi.org/10.1063/1.4967922>.
4. Liang S., Qiao L., Han L. *et al.* Transistor laser with a current confinement aperture in the emitter ridge. *IEEE Electron Device Lett.* 2015. **36**, Issue 10. P. 1063–1065. <https://doi.org/10.1109/LED.2015.2467182>.
5. Taghavi I., Kaatuzian H., Leburton J.-P. Bandwidth enhancement and optical performances of multiple quantum well transistor lasers. *J. Appl. Phys.* 2012. **100**. P. 231114. <https://doi.org/10.1063/1.4727898>.
6. Taghavi I., Kaatuzian H., Leburton J.-P. Performance optimisation of multiple quantum well transistor laser. *IEEE J. Quantum Electron.* 2013. **49**. P. 426. <http://dx.doi.org/10.1109/JQE.2013.2250488>.
7. Lia Y., Leburton J.-P. Base transport factor and frequency response of transistor lasers. *J. Appl. Phys.* 2019. **126**. P. 153103. <https://doi.org/10.1063/1.5099041>.

8. Basu R., Mukhopadhyay B., Basu P.K. Modeling resonance-free modulation response in transistor lasers with single and multiple quantum wells in the base. *IEEE Photonics Journal*. 2012. **4**, No 5. P. 1572–1581. <http://dx.doi.org/10.1109/JPHOT.2012.2211075>.
9. Eladl Sh.M., Saad M.H. Analysis of a quantum well structure optical integrated device. *Semiconductor Physics, Quantum Electronics and Optoelectronics*. 2017. **20**, No 2. P. 204–209. <https://doi.org/10.15407/spqeo20.02.204>.
10. Kaatuzian H., Mojaver H.R., Taghavi I. Optical modulation bandwidth enhancement of heterojunction bipolar transistor lasers using base width variation. *Int. Conf. 2011 Numerical Simulation of Optoelectronic Devices*. 2011. P. 75–76. <https://doi.org/10.1109/NUSOD.2011.6041145>.
11. Tan F., Bambery R., Feng M., Holonyak N., Jr. Transistor laser with simultaneous electrical and optical output at 20 and 40 Gb/s data rate modulation. *Appl. Phys. Lett.* 2011. **99**. P. 061105. <https://dx.doi.org/10.1063/1.3622110>.
12. Tan F., Bambery R., Feng M., Holonyak N., Jr. Relative intensity noise of a quantum well transistor laser. *Appl. Phys. Lett.* 2012. **101**. P. 151118. <https://doi.org/10.1063/1.4760225>.
13. Lenstra D., Fischer A.P.A., Ouirimi A. *et al.* Organic diode laser dynamics: Rate-equation model, reabsorption, validation and threshold predictions. *Photonics*. 2021. **8**, No 7. P. 279. <http://dx.doi.org/10.3390/photonics8070279>.
14. Déziel J.-L., Dubé L.J., Varin C. Dynamical rate equation model for femtosecond laser-induced breakdown in dielectrics. *Phys. Rev. B*. 2021. **104**. P. 045201. <https://doi.org/10.1103/PhysRevB.104.045201>.
15. Ranjan R., Pareek P., Das M.K., Pandey S.K. Numerical design and frequency response of MQW transistor lasers based entirely on group IV alloys. *J. Comput. Electron.* 2021. **20**. P. 1760–1768. <http://dx.doi.org/10.21203/rs.3.rs-164636/v1>.
16. Ramya R., Piramasubramanian S. Effect of Franz–Keldysh absorption on the short optical pulse generation in Transistor Laser. *J. Opt. Commun.* 2020. **474**, No 1. P. 126087. <https://doi.org/10.1016/j.optcom.2020.126087>.
17. Zhang Z., Han H., Tian W. *et al.* A fully stabilized low-phase-noise Kerr-lens mode-locked Yb:CYA laser frequency comb with an average power of 1.5 W. *Appl. Phys. B*. 2020. **126**. Article No 134. <https://doi.org/10.1007/s00340-020-07485-6>.

Authors' contributions

Eladl Sh.M.: conceptualization, methodology, software, validation, formal analysis, investigation, resources, data curation, writing – original draft, writing – review & editing, visualization, supervision, project administration, funding acquisition.

Sharshar K.A.: formal analysis, resources, writing – original draft, writing – review & editing, visualization, supervision, project administration, funding acquisition.
Saad M.H.: investigation, data curation, writing – review & editing, visualization, supervision, project administration, funding acquisition.

Authors and CV



Shaban Marzouk Eladl, Associate Professor in Radiation Engineering Department, Egyptian Atomic Energy Authority (EAEA), Cairo, Egypt. He was born in 1970, received the BS and MS degrees in Electronics and Communications (Electrical Engineering) from Faculty of Electronic Engineering, Menoufia University, Egypt in 1993 and 1999, respectively. In 2004, he received PhD degree in Electronics and Communications (Electrical Engineering) from Faculty of Engineering, Al-Azhar University, Cairo, Egypt. His main areas of research interest are optoelectronics, optical communications, signal processing simulation and modelling. E-mail: shabanmarzouk45@gmail.com; <https://orcid.org/0000-0002-0836-1084>



Karam Amin Ali Sharshar, Professor in Radiation Engineering Department, Egyptian Atomic Energy Authority (EAEA), Cairo, Egypt. He was born in 1955, received the BS and MS degrees in Electronics and Communications (Industrial Electronics) from Faculty of Electronic Engineering, Menoufia University, Egypt in 1974 and 1979, respectively. In 1996, he received PhD degree in Electronics and Communications (Electrical Engineering) from Faculty of Engineering, Al-Azhar University, Cairo, Egypt. His main areas of research interest are in radiation effects in electronic devices and circuits, and microwave communications. <https://orcid.org/0000-0003-1137-7201>



Mohamed H. Saad, Associate Professor in Radiation Engineering Department of the Atomic Energy Authority, Cairo, Egypt. He was born in Egypt in 1982, he received BSc degree with Honor-Very Good grade in communication and electronics engineering from Banha University, Egypt in 2004. He received MS and PhD degrees in Communication and Electronics Engineering from Al-Azhar University, Egypt in 2010 and 2013, respectively. His main areas of research interest are image and signal processing, FPGA, GPU, simulation and modelling. E-mail: m.hassansaad@gmail.com; <https://orcid.org/0000-0001-8370-3614>

Аналіз динамічних характеристик оптичного інтегрованого пристрою в режимі генерації

Sh.M. Eladl, K.A. Sharshar, M.H. Saad

Анотація. У даній роботі чисельно проаналізовано динамічну характеристику оптичного підсилення оптичного інтегрованого пристрою, що складається з гетероперехідного біполярного транзистора (НВТ) та лазерного діода (LD). Цей тип інтегрованого оптичного пристрою має назву транзисторний лазер (TL). Спочатку моделювання починається з розв'язання рівняння для швидкості LD, щоб отримати його передатну функцію. По-друге, загальна передатна функція всієї структури аналізується чисельно. Проаналізовано вплив частоти відсічки НВТ на амплітудну та фазову частотну характеристику. Результати показують, що НВТ сильно впливає на продуктивність пристрою, де вищі значення частоти відсічки НВТ дають нижчу амплітуду в діапазоні низьких частот. На відміну від фазової характеристики, вища частота відсічки НВТ дає вищу фазу. Оскільки ця модель все ще стабільна і забезпечує швидку реакцію та високе оптичне підсилення на високих частотах, її можна використовувати як оптичний підсилювач та оптичний перемикач у дуже високошвидкісних оптичних системах.

Ключові слова: оптичний інтегрований пристрій, лазерний діод, гетероперехідний біполярний транзистор, транзисторний лазер, гетероперехідний біполярний транзисторний лазер, гетероперехідний біполярний світловипромінюючий транзистор.